THE JOURNAL OF PHYSICAL CHEMISTRY A
A JOURNAL OF THE AMERICAN CHEMICAL SOCIETY

pubs.acs.org/JPCA

Article

Triplet States of Cyanostar and Its Anion Complexes

Published as part of The Journal of Physical Chemistry A virtual special issue "Krishnan Raghavachari Festschrift".

Fredrik Edhborg, Axel Olesund, Vikrant Tripathy, Yang Wang, Tumpa Sadhukhan, Andrew H. Olsson, Niels Bisballe, Krishnan Raghavachari, Bo W. Laursen, Bo Albinsson,* and Amar H. Flood*

Cite This: *J. Phys. Chem. A* 2023, 127, 5841−5850

Read Online

ACCESS | Metrics & More | Article Recommendations | Supporting Information

ABSTRACT: The design of advanced optical materials based on triplet states requires knowledge of the triplet energies of the molecular building blocks. To this end, we report the triplet energy of cyanostar (**CS**) macrocycles, which are the key structure-directing units of small-molecule ionic isolation lattices (SMILES) that have emerged as programmable optical materials. Cyanostar is a cyclic pentamer of covalently linked cyanostilbene units that form π-stacked dimers when binding anions as 2:1 complexes. The triplet energies, E_T, of the parent cyanostar and its 2:1 complex around PF_6^- are measured to be 1.96 and 2.02 eV, respectively, using phosphorescence quenching studies at room temperature. The similarity of these triplet energies suggests that anion complexation leaves the triplet energy relatively unchanged. Similar energies (2.0 and 1.98 eV, respectively) were also obtained from phosphorescence spectra of the iodinated form, **I-CS**, and of complexes formed with PF_6^- and IO_4^- recorded at 85 K in an organic glass. Thus, measures of the triplet energies likely reflect geometries close to those of the ground state either directly by triplet energy transfer to the ground state or indirectly by using frozen media to inhibit relaxation. Density functional theory (DFT) and time-dependent DFT were undertaken on a cyanostar analogue, **CSH**, to examine the triplet state. The triplet excitation localizes on a single olefin whether in the single cyanostar or its π-stacked dimer. Restriction of the geometrical changes by forming either a dimer of macrocycles, $(\mathbf{CSH})_2$, or a complex, $(\mathbf{CSH})_2{\cdot}PF_6^-$, reduces the relaxation resulting in an adiabatic energy of the triplet state of 2.0 eV. This structural constraint is also expected for solid-state SMILES materials. The obtained T_1 energy of 2.0 eV is a key guide line for the design of SMILES materials for the manipulation of triplet excitons by triplet state engineering in the future.

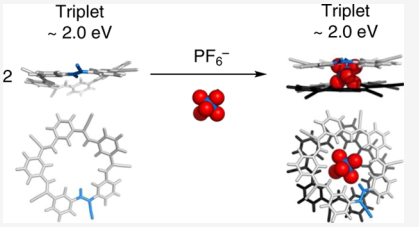

INTRODUCTION

The triplet (T) states of organic molecules[1−3] are integral to the function of materials with advanced optical properties.[4,5] Topical examples include photon upconversion, singlet fission, and thermally activated delayed fluorescence, which are considered potential elements of next-generation technologies for solar energy capture and information processing.[6−14] These materials also rely on the transfer of energy to and from singlet (S) states. Consequently, knowledge of the relative energies of each state and the extent to which these states are modified by packing into high-density solids[15,16] are important fundamental properties. While packing rarely alters triplet states, it often leads to exciton coupling with substantial deterioration in the properties of singlet states.[17−20] Without a strategy to mitigate exciton coupling,[21,22] heavy losses in quantum efficiency are observed. Our recent discovery of small-molecule, ionic isolation lattices (SMILES)[23] produced a reliable strategy to mitigate this coupling. This discovery led to the creation of the brightest nanoparticles[24] and fluorescent materials[25,26] stemming from uncoupled singlet states. Thus, the opportunity for creating materials composed of organic molecules in high-density solids with both well-defined triplet and singlet energies can now be considered. Investigation of this opportunity, however, requires characterization of the triplet energies of SMILES materials.

The construction of SMILES materials relies on charge-by-charge packing[22] of cationic dyes to isolate and decouple them from each other.[27] For this purpose, we use cyanostar macrocycles[28] (**CS**, Figure 1a,b) to bind the dye's counter anion (X^-, Figure 1c) and generate 2:1 anionic complexes. These negatively charged complexes stack into an alternating lattice with the cationic dyes. Thus, the first step to using SMILES as an optical material for manipulating triplet excitation is to determine the triplet energies of the structure-directing cyanostar macrocycles and the anion-bound complexes present in the SMILES lattices.[23] We do this here by using quenching studies, phosphorescence (Phos) spectra, and time-dependent density functional theory (TD-

Received: April 24, 2023
Revised: June 23, 2023
Published: July 10, 2023

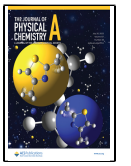

https://doi.org/10.1021/acs.jpca.3c02701
J. Phys. Chem. A 2023, 127, 5841−5850

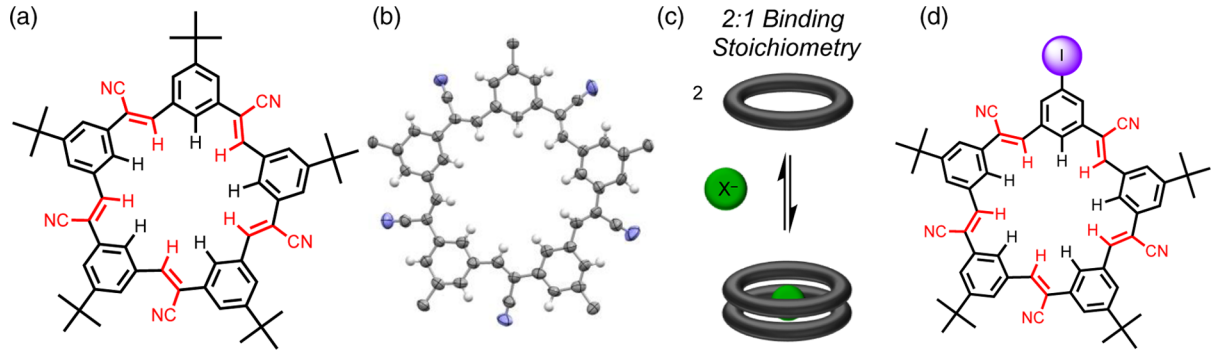

Figure 1. (a) Chemical and (b) crystal structure of cyanostar (**CS**) macrocycles. *tert*-Butyl groups have been removed for simplicity. (c) Preferred binding equilibria of cyanostar as a 2:1 complex around anions (X^-, green) of the right size, e.g., PF_6^-. (d) Chemical structure of iodo-cyanostar (**I-CS**).

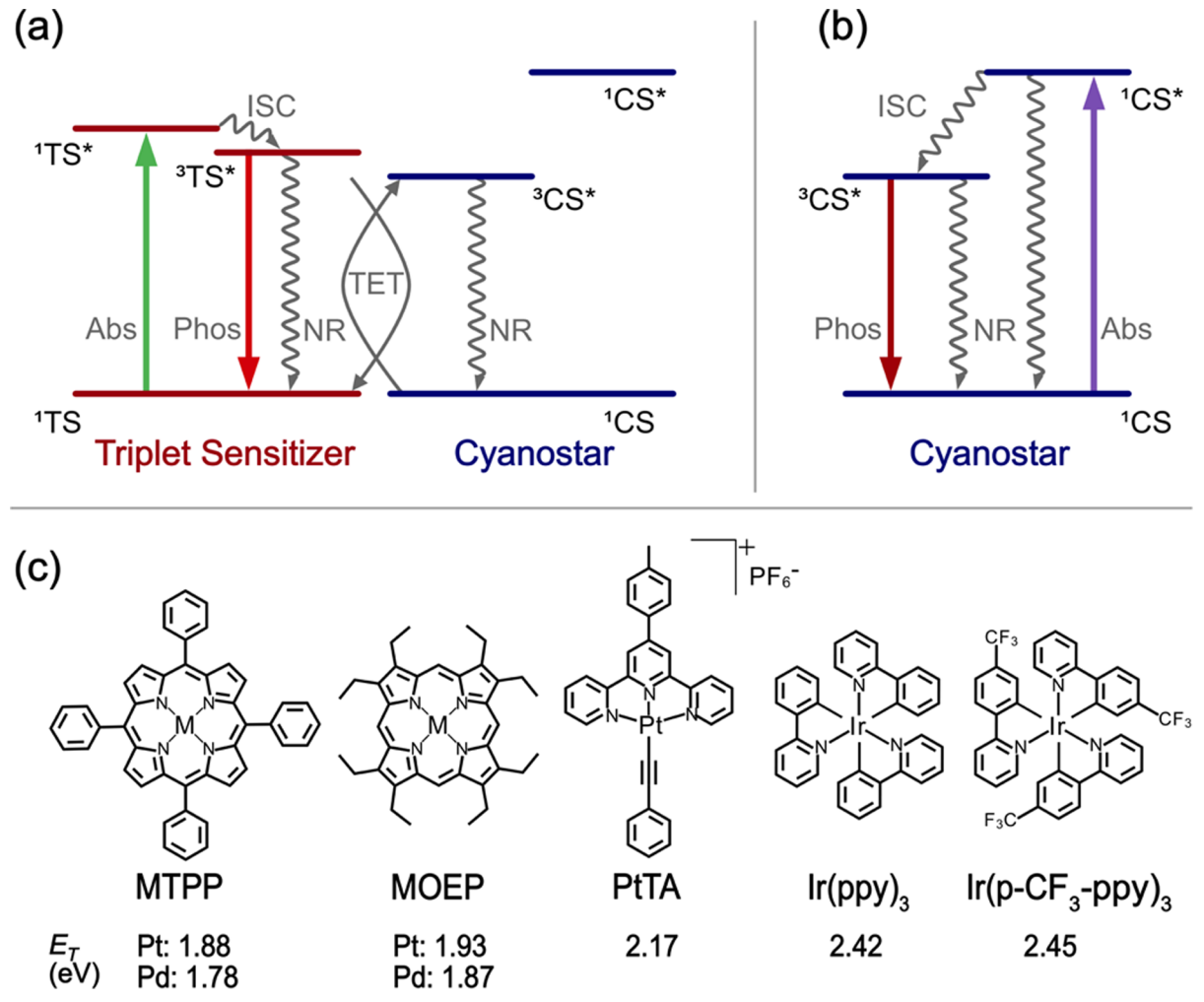

Figure 2. Simplified Jablonski diagrams illustrating the two different methods for determination of the cyanostar triplet energy using (a) Phos quenching with TET from a series of triplet sensitizers (TS) with known triplet state (^{3}TS*) energies, and (b) cyanostar Phos, populating the cyanostar triplet excited state by intersystem crossing (ISC) from the photoexcited singlet excited state (^{1}**CS***). Photophysical processes shown are absorption (Abs), Phos, and nonradiative deactivation (NR). (c) Molecular structures of triplet donors; M = Pd, Pt for MOEP and MTPP.

DFT) to show that the triplet energy of cyanostar and its anion-driven complexes are both around 2.0 eV.

The chromophoric units in the cyanostar are five *trans*-cyanostilbenes. Stilbene and its derivatives have been thoroughly studied and they are the archetypical cis−trans isomerizing olefins.[29] These compounds often display twisted excited states and are subject to conformational heterogeneity.[30,31] The lowest photoexcited triplet state energies for many monomolecular stilbene derivatives have been reported both from triplet energy transfer (TET) experiments as well as Phos in low-temperature glasses;[32] however, no literature was found reporting the excited triplet energy for the specific *trans*-cyanostilbene derivative present in cyanostar.

https://doi.org/10.1021/acs.jpca.3c02701
J. Phys. Chem. A 2023, 127, 5841−5850

The triplet states of cyanostar have not previously been measured. The cyanostar macrocycle, its anion-binding properties,[28,33−36] and its packing in SMILES crystals have been well described.[23,24] The parent cyanostar is monomolecular in solution. It displays rapid interconversion between ∼300 low-energy conformations as revealed by molecular dynamics, DFT, and confirmed using the nuclear Overhauser effect.[37] The cyanostar has five cyanostilbenes in cross-conjugation with each other. Consistent with the optical spectroscopy of cyanostilbene,[38] cyanostar displays a low-quantum yield fluorescence band at 410 nm (3.3 eV) at room temperature.[23] Upon binding size-matched anions, like PF_6^-, it forms a discrete 2:1 complex.[28] In this form, the two macrocycles are π-stacked and display a ∼36° rotational offset from each other on account of interlocking steric contacts defined by the five *tert*-butyl substituents. While the number of conformations is reduced in the complex, it retains thermal access to many local minima with dynamically varying torsion angles indicative of a relatively flexible ground state.[37,39] Nevertheless, the stability of the 2:1 anion complex with the PF_6^- anion is remarkably high, recorded at 10^{12} M^{-2}. The stability of this complex, $\mathbf{CS}_2{\cdot}PF_6^-$, is generally accepted to increase in less polar solvents, like dichloromethane (DCM).[34,40] When studying anion binding, a spectroscopically and redox-inert cation such as tetrabutylammonium (TBA^+) is typically used. Further lowering of the solution polarity drives favorable ion pairing of the anionic 2:1 complexes with the counter cation.[41] Chloroform and aromatic solvents typically support these tight ion pairs.[35,41] The resulting 2:1:1 species, $\mathbf{CS}_2{\cdot}PF_6{\cdot}$TBA, is the elementary unit of crystal structures observed with various anions. They are also the units that compose the SMILES materials where the inert cations are replaced with optically active dyes.[23] Thus, the triplet energies of the 2:1 and 2:1:1 building blocks are key to laying the groundwork for designing triplet-based optical materials.

Herein, we describe an experimental and computational study of the first excited triplet state energies of cyanostar and its 2:1 cyanostar-anion complexes. Phos quenching (Figure 2a) using a Sandros analysis[42] was used to estimate the triplet excited state energies of cyanostar (1.96 eV) and the corresponding anionic complex (2.02 eV) revealing an insignificant change in the triplet energies upon complexation. The triplet energies (2.0 eV) match the one measured using Phos (Figure 2b) from cyanostar and its iodo-substituted variant (iodo-cyanostar, **I-CS**, Figure 1d) in low-temperature glasses. Both processes likely probe transitions between structurally similar S_0 and T_1 states. Computational studies using DFT and TD-DFT were performed to complement the experimental results and investigate the geometry of the cyanostar in the ground and excited states. This study is the first exploration into the triplet state and Phos properties of cyanostar and lays the foundation for the design of SMILES materials exploiting the triplet manifold.

METHODS

The synthesis of PtTA was based on established procedures. Stern−Volmer analyses conducted for the Phos quenching studies were performed in tetrahydrofuran (THF) at room temperature. Phos spectra of cyanostar and its complexes were measured in 2-methyltetrahydrofuran (MeTHF) at 85 K. DFT calculations have been performed to investigate the geometries and electronic states of the parent cyanostar as well as some of its relevant associated species. Structures were optimized at the B3LYP-D3BJ/6-31G level of theory for the cyanostar, **CSH**, its dimer, $(\mathbf{CSH})_2$, and the 2:1 complex, $(\mathbf{CSH})_2{\cdot}PF_6^-$. Single point calculations were performed on the optimized geometries using CAM-B3LYP-D3BJ/6-31+G(d). A CPCM continuum solvation model was used. For further details, please refer to the Supporting Information.

RESULTS AND DISCUSSION

Determining the Triplet Energy of Cyanostar Using Phos Quenching. The triplet energy of a molecule can be determined by measuring the rate constant of TET from a triplet donor of known triplet energy, the so-called Sandros method.[42] Assuming dynamic, diffusion-mediated energy transfer, the rate constant of TET, k_{TET}, depends on the energy difference between the triplet excited state of the donor, $E_{T,D}$, and the acceptor, $E_{T,A}$, as described by the Sandros equation

$$k_{TET} = \frac{k_{diff}}{1 + \exp(-(E_{T,D} - E_{T,A})/k_B T)} \quad (1)$$

Here, k_B is the Boltzmann constant, T is the temperature, and k_{diff} is the diffusion-controlled rate of collision between donor and acceptor. Equation 1 shows that k_{TET} approaches k_{diff} when the energetic driving force of TET increases, but k_{TET} decreases exponentially when $E_{T,A} > E_{T,D}$, i.e., when TET from the donor to acceptor is energetically uphill.

Using a set of triplet energy donors (Figure 2c) with a range of known triplet energies, the unknown triplet energy of an acceptor can be determined from the measured k_{TET} rate constants after fitting to the Sandros equation (eq 1). If the donor molecules are phosphorescent, the rate of TET can be calculated from the Phos intensity (or Phos lifetime) of the donor, measured in absence (I_0, τ_0) and in the presence of the acceptor (I, τ). The rate constant of TET, k_{TET}, is calculated by assuming dynamic quenching and using the Stern−Volmer relationship (eq 2), where $[A]$ is the concentration of the acceptor.

$$\frac{I_0}{I} = \frac{\tau_0}{\tau} = 1 + \tau_0 k_{TET}[A] \quad (2)$$

Rate constants of TET to cyanostar, **CS**, and its anion complex $\mathbf{CS}_2{\cdot}PF_6^-$, were measured using a series of phosphorescent triplet energy donors, including four metal porphyrins, two iridium(III) complexes and a platinum(II) complex (Figure 2c). The donor molecules platinum(II) octaethylporphyrin (PtOEP), palladium(II) octaethylporphyrin (PdOEP), platinum(II) tetraphenylporphyrin (PtTPP), palladium(II) tetraphenylporphyrin (PdTPP), *tris*(2-phenylpyridine)iridium(III) [$Ir(ppy)_3$], *tris*(2-*p*-trifluoromethylphenylpyridine)iridium(III) [$Ir(p\text{-}CF_3\text{-}ppy)_3$], and platinum(II) terpyridylphenylacetylide (PtTA) have triplet energies spanning from 1.7 to 2.4 eV, as determined from the peak or onset of their Phos emission (see the Supporting Information for details). This range of triplet energies were found to span the expected triplet state energy of cyanostar, thereby allowing the Sandros method to accurately determine its triplet energy.

The measured values of k_{TET} for cyanostar, **CS**, and its complex, $\mathbf{CS}_2{\cdot}PF_6^-$, as a function of the donor energies can be plotted versus the donor triplet energies (Figure 3). All Phos quenching measurements were performed in THF, except for the PtTA which was conducted in DCM on account of

https://doi.org/10.1021/acs.jpca.3c02701
J. Phys. Chem. A 2023, 127, 5841−5850

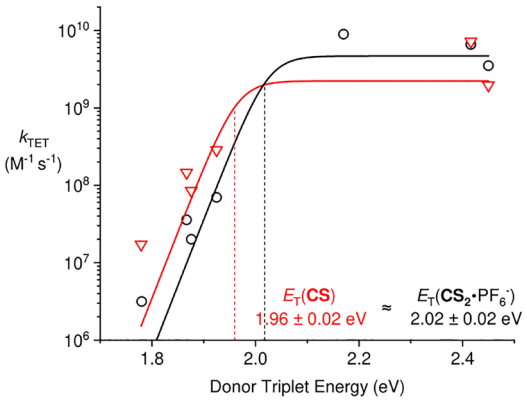

Figure 3. Sandros plots associated with the **CS** macrocycle (red triangles) and its anionic complex $\mathbf{CS_2}\cdot PF_6^-$ (black circles) using PtOEP, PdTPP, PtTPP, PdTPP, Ir(ppy)$_3$, and Ir(p-CF_3-ppy)$_3$ in THF and using PtTA in DCM as energy donors. Donor concentration was approximately 5−10 μM with the cyanostar concentration ranging from 10 to 500 μM for the generation of the Stern−Volmer quenching plots (SI). Solid lines show fits to eq 1.

solubility. Each data point corresponds to a series of Phos quenching experiments (see Stern−Volmer plots, Figures S2 and S3 and Table S1). For the mono-molecular cyanostar, **CS**, the best fit to eq 1 gives a triplet energy of 1.96 eV ± 0.02 eV. Here, the error is obtained from the data fitting. The estimated triplet energy of cyanostar is similar to the triplet energy of *trans*-stilbene,[32,43] indicating weak electronic communication on the triplet surface between the five meta-connected cyanostilbene subunits making up the cyanostar molecule. Using the same method, the triplet energy of the corresponding 2:1 complex, $\mathbf{CS_2}\cdot PF_6^-$, was estimated to be 2.02 ± 0.02 eV from the fitted data (Figure 3). The minor and insignificant change in triplet energy upon anion-driven dimerization is consistent with the minor anion-induced change seen in the UV−vis Abs spectrum.[28] It should be noted that the error presented for these numbers is the standard error of fitting and should not be considered as the accuracy of the received triplet energy value. A rough estimate of the accuracy can instead be achieved by iteratively fitting the data in the Sandros plots (Figure 3) with a fixed value of the triplet energy to study how much the triplet energy can be varied and still result in a reasonable fit. With this simple method, the accuracy of the determined triplet energy is estimated to be ±0.05 eV. Further discussion about the accuracy of the method is given below.

Phos from Cyanostar. To provide an independent measure of the triplet energy of the cyanostar and its anion complex, we also measured their Phos spectra, which gives a more direct readout of the triplet energy. Similar to *trans*-stilbene, the cyanostar itself is not phosphorescent in liquid solution at room temperature but becomes very weakly phosphorescent in a low-temperature glass and in the presence of a heavy atom.[43] The low-temperature glass is expected to freeze out the conformational dynamics, whether they involve local distortions in the ground state as seen by MD[37] or twisting in the excited states. The glasses also inhibit bimolecular quenching from residual oxygen. As a result, we expect to increase Phos by lowering the rate of non-radiative decay from the triplet state (Figure 2b). We also expect the cyanostar to be frozen into a distribution of conformations at low temperature. Prior DFT studies[37] showed us that the cyanostar is not perfectly flat but instead has access to various conformations. In each of these, the cyano-olefin groups tilt either above or below the macrocycle's mean plane. The most stable conformations of the cyanostar have two non-neighboring olefins tilted above the plane and three below (Figure 4a). There are multiple combinations of this ruffled

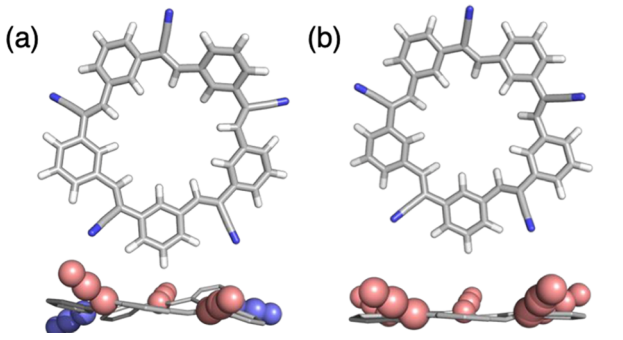

Figure 4. (a) Lowest-energy conformation of the cyanostar monomer. (b) Lowest energy conformation of one of the cyanostar macrocycles within a 2:1 cyanostar complex around a diglyme guest molecule. Geometries calculated with DFT as described previously.[37]

conformation for an overall 10-fold degeneracy. Based on Boltzmann statistics, there is ∼9% population in each of the 10 conformers at 85 K. Higher-energy conformations (totaling 10%) have similar tilts but across different combinations of olefins. In total, there is a high degree of conformational heterogeneity in the cyanostars. When examined in the complex, when two macrocycles are π stacked, the preferred conformation changes (Figure 4b) and while the number of conformations reduce, they are still plentiful in number.

In this study, two different approaches were used to induce Phos in the cyanostar. First, we covalently substituted the macrocycle with iodine[44] to make iodo-cyanostar (**I-CS**, Figure 1). Second, we leveraged cyanostar's facility for anion binding to use periodate, IO_4^-, in the formation of a 2:1 anion complex.[28] The iodine atoms were used as a means to exploit the heavy atom effect to enhance ISC and thereby increase the population of the triplet excited states from the photoexcited singlet excited state (Figure 2b), as well as to enhance the rate of Phos.[45] In the case of IO_4^-, this anion provided a non-covalent mechanism of influencing ISC. Spectra were recorded for the mono-molecular iodo-cyanostar, the anion complex of **I-CS** using the non-heavy atom PF_6^- anion, $(\mathbf{I\text{-}CS})_2\cdot PF_6^-$, and a dimer of the parent cyanostar with a periodate anion, $\mathbf{CS_2}\cdot IO_4^-$. All measurements were performed at 85 K in a frozen organic glass of MeTHF. Under these conditions, we assume **I-CS** to be frozen into 10+ conformations with the cyano groups tilted above and below the ring (vide supra). In the complexes, the conformational landscape is far simpler. All 10 cyano groups on both cyanostars are tilted away from the π-stacked seam (Figure 4b). In both the complexed and uncomplexed cyanostars, the low-energy barriers seen by MD (1.5 kcal/mol) suggest that there will be a distribution of many different tilt angles in the low-temperature glasses. We also assume that formation of contact ionpairs, e.g., $\mathbf{CS_2}\cdot IO_4$·TBA, will be favored on entropic grounds as the temperature is lowered down to the glass transition temperature of MeTHF (137 K) and ultimately in the glass.

The Phos spectra of the iodinated cyanostar and the anion complexes (Figure 5) were recorded using time-gated

https://doi.org/10.1021/acs.jpca.3c02701
J. Phys. Chem. A 2023, 127, 5841−5850

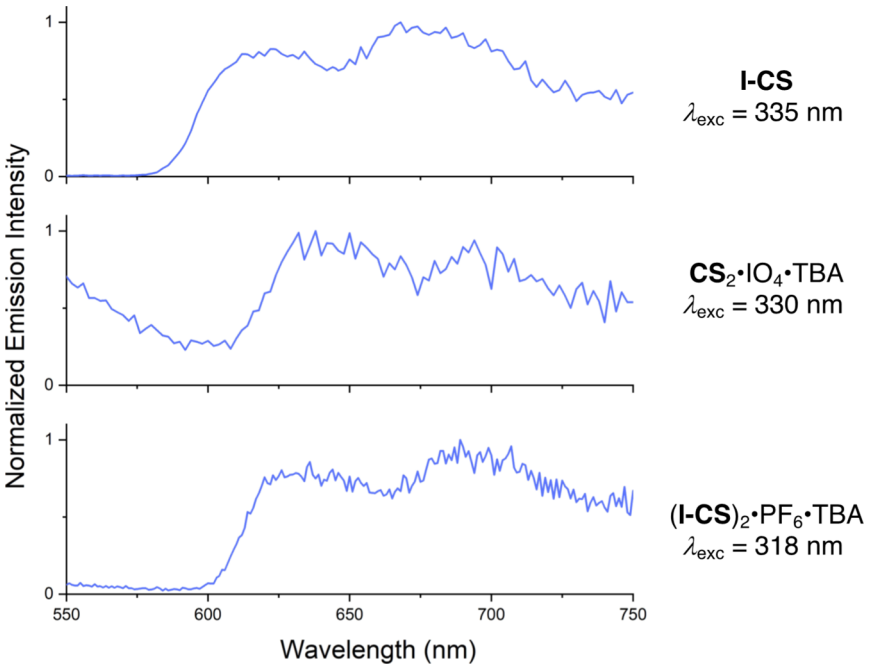

Figure 5. Phos spectra of **I-CS**, $\mathbf{CS_2}$·IO_4·TBA, and $(\mathbf{I\text{-}CS})_2$·PF_6·TBA. Spectra recorded in MeTHF (~20−40 μM) at 85 K at various excitation wavelengths as noted.

emission. Therein, the sample is excited with a short excitation pulse and the emission signal is recorded after a time delay in order to exclude any short-lived emission signals like fluorescence. The emission spectrum of **I-CS** (Figure 5) shows clear Phos in the region of 600−750 nm with two resolved vibronic bands centered at 620 and 675 nm. The triplet energy level is estimated from the position of the highest energy Phos band (620 nm), which corresponds to 2.0 eV. The emission spectra of the anion-induced dimers, $\mathbf{CS_2}$·IO_4·TBA and $(\mathbf{I\text{-}CS})_2$·PF_6·TBA show Phos in the same region with two vibronic bands, but with lower intensity and lower signal-to-noise ratio. The energy of the highest-energy Phos band (635 and 625 nm) for $\mathbf{CS_2}$·IO_4·TBA and $(\mathbf{I\text{-}CS})_2$·PF_6·TBA, respectively, corresponds to a triplet energy of 1.95 and 1.98 eV. The emission intensity seen at shorter wavelengths for $\mathbf{CS_2}$·IO_4·TBA and $(\mathbf{I\text{-}CS})_2$·PF_6·TBA is assigned to the tail of the strong fluorescence which could not be eliminated totally in the gated emission. This interpretation is supported by the close spectral resemblance of the emission tail in the 500−600 nm region and the steady-state fluorescence spectrum (Figure S4). Low-intensity Phos precluded measurements of the quantum yields. The Phos emission decay was measured (Figure S5) for **I-CS** and $(\mathbf{I\text{-}CS})_2$·PF_6·TBA but could not be measured for $\mathbf{CS_2}$·IO_4·TBA stemming from the lower emission intensity. The Phos decay could be fitted to a biexponential decay with an average lifetime (amplitude weighted) of 0.50 ms for **I-CS**, and 0.30 ms for $(\mathbf{I\text{-}CS})_2$·PF_6·TBA (Table S2).

The estimates of the triplet energies are closely matched. The Phos spectra of the two different cyanostar complexes (Figure 5) are similar, which suggest that iodine substitution only adds a small (~30 meV) perturbation to the triplet energy. The triplet energies of cyanostar determined from the Phos spectra match with the triplet energy of substituted stilbenes, E_T ~ 2.0 eV.[32] This resemblance suggests that the meta linkage between the five cyanostilbenes present in the cyanostar leads to triplet states localized on one stilbene unit as supported from calculation. The close resemblance between the measured triplet energies of the cyanostar monomer and its anion complex, from both the emission quenching and Phos experiments, show that π-stacked dimerization of the cyanostar only induces a minor shift in the triplet energy.

The triplet energy estimated from quenching studies matches low-temperature Phos despite probing different processes (Figure 2a,b). The first is a Dexter energy-transfer excitation from the singlet ground state of cyanostar to its first triplet excited state, while the second is a radiative decay from the excited triplet state of the cyanostar that is likely frozen in a ground state-like geometry. Given the matching energies, both processes likely probe transitions between similar S_0 and T_1 states with modest geometrical distortion between them.

Even though both methods give very similar estimates of the triplet energies, the accuracy of the two methods needs to be considered. The accuracy of the Sandros method depends on how well the triplet energies of the donors have been determined as well as the accuracy in the estimation of the rate constant of TET derived from the Phos quenching experiments. Furthermore, the Sandros method assumes free diffusion of both the donor and acceptor and that all donors−acceptor pairs share the same diffusion limited rate constant of energy transfer, k_{diff}. More donor molecules could, of course, be included in the study to get more data points in the Sandros plot. However, the six or seven donors included in this study are considered sufficient to provide an estimate of the cyanostar-based triplet energies. As already noted, these donors span a suitable range of triplet energies. This range enables access to a rate constant close to the diffusion limit[1] for TET of ~5×10^9 M^{-1} s^{-1} when $E_{T,A} < E_{T,D}$ and to triplet energies giving a TET rate constant that is 2 or 3 orders of magnitude lower when $E_{T,A} > E_{T,D}$.

The Phos spectra of the cyanostar gives an estimate of the triplet energy of the molecule in a solid environment at low temperature likely locked in a ground state-like geometry. This situation could be quite different from a fully relaxed triplet state obtained in liquid solution at room temperature. For the

https://doi.org/10.1021/acs.jpca.3c02701
J. Phys. Chem. A 2023, 127, 5841−5850

Table 1. Experimental Triplet Energies Obtained from Various Forms of the Cyanostar in Various Physical States

compound	solvent	state	T/K	E_T/eV	τ/ms[a]	experiment[b]
CS	THF	liquid	RT	1.96 ± 0.05		TET
$CS_2{\cdot}PF_6^-$	THF	liquid	RT	2.02 ± 0.05		TET
I-CS	MeTHF	glass	85	2.0	0.50	phos
$CS_2{\cdot}IO_4{\cdot}TBA$	MeTHF	glass	85	1.95		phos
$(\textbf{I-CS})_2{\cdot}PF_6{\cdot}TBA$	MeTHF	glass	85	1.98	0.30	phos

[a]Average lifetime (amplitude weighted). [b]Measured using TET by Stern−Volmer quenching of triplet states (1.78−2.45 eV) according to the Sandros method. Uncertainties determined from a sensitivity analysis. Phos experiments conducted using time-gated emission.

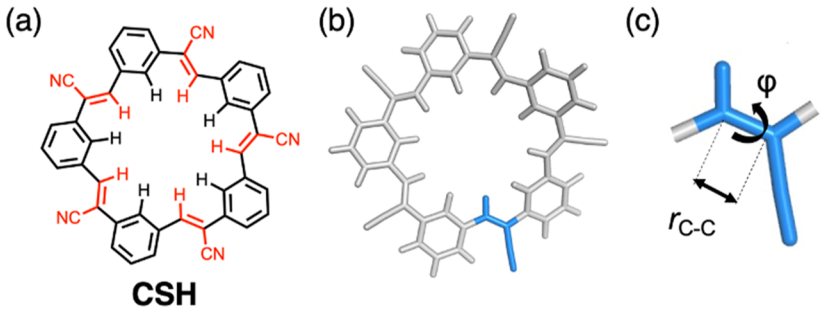

Figure 6. (a) Structure of modified cyanostar (**CSH**). (b,c) Definition of the torsion angle and the C═C bond coordinate that deform in the excited states of cyanostar and its complexes.

quenching studies the experimental situation is quite different, but is also expected to involve **CS** and $CS_2{\cdot}X^-$ complexes in ground state geometries.[46] Thus, geometry relaxation of the T_1 state is highly prohibited in both cases (though for different reasons), which may explain the close match of the triplet energies between the two methods (Table 1). From this argument, we conclude that the triplet excited state energy of both the cyanostar and its anion complexes is close to 2.0 eV when major geometry changes are prohibited. This situation also corresponds to the cyanostar complexes in SMILES materials. Thus, this T_1 energy is relevant for the design of SMILES materials that incorporate phosphorescent dyes and for the manipulation of triplet excitons.

Calculations on the Singlet and Triplet Excited States. DFT calculations were performed to investigate the electronic states of the parent cyanostar and its complexes as well as the structure of the excited states that were not probed experimentally. TD-DFT was employed to obtain excited singlet state properties including the excitation and emission energies along with the associated oscillator strengths. The *tert*-butyl groups of cyanostar were replaced with hydrogen atoms in the model compound **CSH** (Figure 6a) to reduce the computational cost at very little loss in accuracy.

Structures were optimized at the B3LYP-D3BJ/6-31G level of theory for the cyanostar, **CSH**, its dimer, $(\textbf{CSH})_2$, and the 2:1 complex, $(\textbf{CSH})_2{\cdot}PF_6^-$. Polarization functions were added to the anion to accommodate the hypervalent phosphorous atom. Single-point calculations were performed on the optimized geometries using CAM-B3LYP-D3BJ/6-31+G(d). DCM (ε = 8.93) was used as the solvent in conjunction with a CPCM continuum solvation model. This model should be representative of low polarity solvents. A modest change in solvent polarity, such as for THF (ε = 7.58), is expected to have insignificant impact on our results.

The behavior of the ground state singlet (S_0) of **CSH** has been analyzed previously.[37] There are many low-lying conformers (332) within a small energy window (2.3 kcal/mol) undergoing rapid interconversion. Each of them has a ruffled semi-planar geometry. The deviation from planarity stems from non-zero dihedrals in the C−C single bonds connecting the phenylene units and the olefin units. In the ground state of the cyanostar and its complexes, the olefin's C═C double bond (defined in blue, Figure 6b,c) is mostly untwisted with a dihedral angle close to ∼0° (varying between 0 and 5° in the different conformations). Despite these small deviations from planarity and the conformational heterogeneity, **CSH** is shape persistent as a result of the relatively small average change in molecular geometry across these conformations.[37] Considering both the pseudo-degenerate character of the 332 ground state conformers (relative to the typical scale of electronic states, ∼50 kcal/mol) and the macrocycle's shape persistence, the effect of these conformers on the energies of the various singlet and triplet states is assumed to be negligible in our current work.

The optical Abs was examined using the ground state geometry (Figure 7a). The cyanostar structure has pseudo-five-

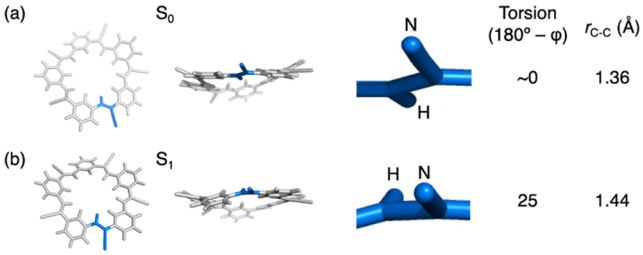

Figure 7. Structural characteristics of the (a) S_0 and (b) S_1 states obtained by DFT and TD-DFT, respectively.

fold symmetry, and it is convenient to consider the behavior expected from C_5 symmetry. Analysis of the first five excited states shows that the first excited state, S_1, is non-degenerate, while the second and third excited states, S_2 and S_3, are close in energy (pseudo-degenerate), as are the S_4 and S_5 states. The excitation energy corresponding to the $S_0 \rightarrow S_1$ transition is 3.6 eV albeit with a low oscillator strength (f = 0.004). The S_2 and

https://doi.org/10.1021/acs.jpca.3c02701
J. Phys. Chem. A 2023, 127, 5841−5850

S_3 states lie at 3.8 eV with very high oscillator strengths (f = 2.2). This finding is consistent with the lowest-energy UV−vis Abs maximum of **CS** measured at 3.8 eV. The S_4 and S_5 states lie at 3.9 eV with small oscillator strengths (f = 0.04 and 0.02, respectively).

The rate of internal conversion from S_2 to S_1 is usually rapid and emission is therefore expected to occur from the S_1 state. Thus, geometry optimization of the S_1 state was carried out using TD-DFT (see the Supporting Information for details). Compared to the geometry of the S_0 state (Figure 7a), the optimized geometry of the cyanostar in its S_1 state (Figure 7b) shows one of the five olefins is twisted from 0 to 25° and the double bond is elongated from 1.36 to 1.44 Å. This change in geometry is similar to half the elongation from a double bond (1.34 Å in ethylene) to a single bond (1.54 Å in ethane) suggesting a bond order of 1.5. The transition energy for emission from this S_1 state to the S_0 state (at the S_1 geometry) is found to be 2.9 eV. This finding is consistent with the fluorescence spectral maximum of **CS** observed at ∼3.0 eV. Thus, the calculated singlet manifolds are consistent with experimental observations.

Unlike fluorescence, Phos originates from an excited state of different spin symmetry (triplet, T) and can be calculated directly using standard ground-state DFT methods. As a model of the possible features we might expect, it is common for stilbenes to be twisted about the C═C double bond in the excited state, consistent with the expected cis−trans isomerization.[47] An analogous feature becomes prominent in the triplet state of the mono-molecular **CSH** (Figure 8a). Therein,

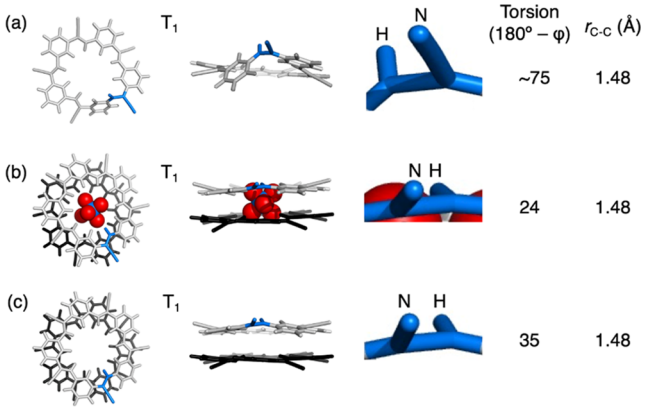

Figure 8. Structural characteristics of the triplet (T_1) states of (a) **CSH**, (b) the anion complex $(\mathbf{CSH})_2{\cdot}PF_6^-$, and (c) cyanostar dimer $(\mathbf{CSH})_2$ obtained by DFT.

the triplet state shows a substantial ∼75° twisting about a C═C double bond in one of the five cyanostilbene units. Such a state has an adiabatic energy difference between excited triplet (T_1) and ground (S_0) state at their respective geometries of 1.7 eV. However, the geometry change is so large that it will have very little Franck−Condon overlap with the ground state.

The Phos studies were carried out at low temperature (85 K) in a glassy solid, which will restrict movements in the cyanostar, like twisting. We expect the pseudo-rigid environment of the glass to be replicated in the calculated 2:1 complex $(\mathbf{CSH})_2{\cdot}PF_6^-$ (Figure 8b), which has been studied experimentally as $(\mathbf{CS})_2{\cdot}PF_6^-$. In this case, reduced twisting in the calculated structure likely emerges from a combination of the steric constraints of the adjacent macrocycle and the sum of stabilizing interactions from the π stacking and the CH···PF_6^- hydrogen bonding counteracting the tendency to rotate. We observe (Figure 8b) a reduction in the triplet's twist angle to only 24°. The adiabatic energy is now calculated to be 2.0 eV, some 0.3 eV higher than the triplet state of **CSH**. The less twisted triplet state of $(\mathbf{CSH})_2{\cdot}PF_6^-$ likely has a more reasonable Franck-Condon overlap with the ground singlet state.

In order to further model the uncomplexed cyanostar in the absence of the anion, we carried out two sets of studies. In the first, we studied the geometry of the stacked cyanostar dimer, $(\mathbf{CSH})_2$ (Figure 8c). This species is not necessarily expected to be present in solution but serves as a surrogate to replicate the steric constrains imposed by other species, like the glassy solvent. The dimer was obtained by removing the anion from the complex and reoptimizing the geometry. Again, the twisting is smaller (only 35°) than the single macrocycle, but it retains the 0.12 Å extension in the olefin. The energy of this triplet is at 1.9 eV, showcasing again how the degree of shape change correlates with the triplet energy. Further analysis of the character of the triplet excited state in this stacked cyanostar dimer $(\mathbf{CSH})_2$ shows the excitation is almost completely localized on one of the two cyanostar macrocycles. The other macrocycle is playing a passive role with respect to the electronic excitation. When the passive cyanostar is removed, the distorted cyanostar again shows a triplet energy close to 2.0 eV. If, however, it is allowed to relax, it forms the highly twisted triplet seen earlier in the isolated cyanostar (Figure 8a).

Calculations show that less twisted T_1 states of $(\mathbf{CSH})_2$ and $(\mathbf{CSH})_2{\cdot}PF_6^-$ have triplet energies close to 2 eV and that twisting correlates with lowering of the triplet energy. Since the glassy solvent restricts rotation, such a state could explain the experimental observations in the parent cyanostar too. In order to study the properties of a pseudo-planar triplet state, we carried out a potential energy scan to explore the dependence of the triplet energy on the most relevant geometrical parameters. A comparison of S_0 and T_1 geometries reveals that the most significant geometry change occurs only in a few coordinates (Figure 9, R_1, R_2, $r_{C=C}$, and φ). The change in the

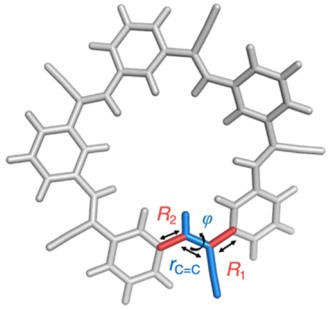

Figure 9. Bonds and dihedral angle next to the C═C bond in the stilbene unit undergoing rotation also change. All the coordinates undergoing significant change are highlighted.

three neighboring bond lengths are correlated with each other. As $r_{C=C}$ increases (by 0.12 Å) on going to the triplet state, both R_1 and R_2 decrease (by 0.05−0.06 Å), consistent with the conjugation across the three bonds.

We performed a stepwise relaxation along the triplet T_1 state from the ground state (S_0) geometry to the pseudo-planar triplet state by fixing the dihedral φ and relaxing the other

https://doi.org/10.1021/acs.jpca.3c02701
J. Phys. Chem. A 2023, 127, 5841−5850

three structural parameters. The scan involved 10 geometrical steps in **CSH** (Figure 10).

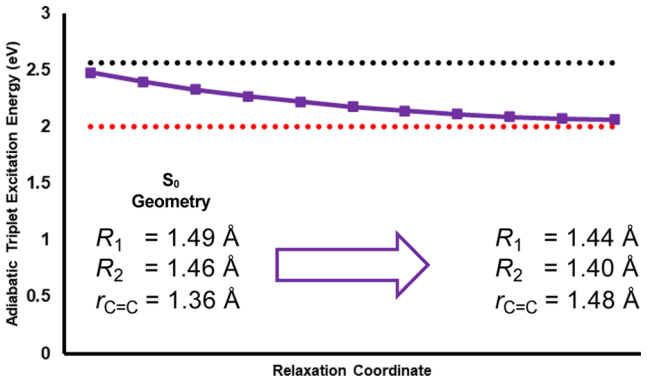

Figure 10. Stepwise relaxation from ground state (S_0) geometry to pseudo-planar triplet geometry of **CSH**, obtained by freezing the dihedral φ. 10 steps were taken, each changing each of the three coordinates by a tenth of the range. At each point, triplet state is optimized while keeping R_1, R_2, $r_{C=C}$, and φ fixed.

The relaxation of R_1, R_2, and $r_{C=C}$ without twisting brings the triplet state down to 2.06 eV, which is close to the experimental value. Restriction in the twisting also shows this state is higher in energy relative to the twisted form of **CSH** by 0.36 eV. It is interesting to note that the terminal (C_1-C_4) bond distance between neighboring phenylene units is changed very little (<0.01 Å) in this scan, due to the opposing effects of the different bond lengths. Thus, the final constrained triplet geometry is changed very little from the ground state geometry. Consistently, we observe that the energy of the untwisted **CSH** triplet (2.06 eV) closely matches that of the $(\mathbf{CSH})_2{\cdot}PF_6^-$ triplet (2.0 eV). This similarity matches the triplet energies measured using the low-temperature Phos in the glassy solids for **I-CS** (2.0 eV) and $(\mathbf{I\text{-}CS})_2{\cdot}PF_6{\cdot}$TBA (1.98 eV).

The results from our calculations are consistent with the findings from both types of experiments reported in this study. The TET (Figure 2a) is related to a vertical excitation from a ground-state cyanostar geometry, ^{1}**CS**, to a triplet state, ^{3}**CS*** (with similar geometry). For the Phos, it involves vertical de-excitation from cyanostar in an excited triplet state. However, its geometry is expected to closely resemble the ground state in the frozen glass on account of restricted motions in this physical state. Thus, both processes likely probe transitions between states with ground state-like geometries, consistent with their matching triplet energies at ∼2.0 eV. This consistency extends to the similar 2.0 eV triplet energy for the single macrocycle and the complexes. The only reasonable explanation for the observation is that Phos from these two forms of the cyanostar are the same is that their geometries are also the same. This interpretation can be best accommodated if the geometries both resemble those of the ground states.

In summary, the DFT studies show that large differences in the triplet energies determined using TET and low-temperature Phos will only occur if there are large-scale geometry changes. Thus, as also shown by the DFT studies, reductions in large scale motions, whether by complexation or increased viscosity, raise the triplet energy. The observations from experiment indicate that the differences in triplet energies measured using the different methods and between the various forms of the cyanostar are negligible. For this reason, the triplet states of cyanostar and its complexes that are populated by TET closely resemble the ground state geometry. Furthermore, the triplet states that are populated in low-temperature glasses also resemble the ground state geometry.

CONCLUSIONS

The triplet energy of both cyanostar and its anion-bound complexes is 2.0 eV when probed using experiments that correspond closely to their ground state geometries. This energy was observed using room-temperature TET quenching studies, which effectively excite the molecules from their ground states to the first triplet state. The same energy was observed using low-temperature (85 K) Phos, which corresponds to light emission from the first triplet state frozen into the ground-state geometry. Therefore, both processes likely probe transitions between S_0 and T_1 states that are in similar ground-state geometries. DFT and TD-DFT provided insights into the role of relaxation on the triplet energy. Full relaxation of a single cyanostar shows a triplet energy of 1.7 eV with one of the olefins twisted and elongated. Upon formation of a 2:1 anion complex, relaxation remains localized on one olefin with the degree of twisting much reduced from 75 to 24° and resulting in a higher 2.0 eV energy for the triplet state. In addition, iodination had a minor effect on the triplet energies while improving the phosphorescent intensity consistent with the heavy atom effect. Use of heavy-element anions like periodate, IO_4^-, was also explored as a means to enhance ISC though the covalently incorporated iodine atom had a more substantial effect. These findings indicate that the primary mode of anion-induced packing of cyanostar macrocycles seen in solid-state SMILES materials has a major impact on the triplet energies by preventing large structural relaxation. These findings provide a blueprint for triplet state engineering in cyanostar-based SMILES defined by a 2.0 eV triplet window in structurally constrained SMILES materials.

ASSOCIATED CONTENT

Supporting Information

The Supporting Information is available free of charge at https://pubs.acs.org/doi/10.1021/acs.jpca.3c02701.

Atomic coordinates for **CSH** S_0 (XYZ)

Atomic coordinates for **CSH** S_1 (XYZ)

Atomic coordinates for the **CSH** triplet (XYZ)

Atomic coordinates for the $(\mathbf{CSH})_2{\cdot}PF_6^-$ triplet (XYZ)

Synthesis of PtTA, Phos quenching data, Stern−Volmer plots, Phos spectra, computational chemistry methods, energies, and atomic coordinates (PDF)

Atomic coordinates for the $(\mathbf{CSH})_2$ triplet (XYZ)

AUTHOR INFORMATION

Corresponding Authors

Bo Albinsson − *Department of Chemistry and Chemical Engineering, Chalmers University of Technology, Gothenburg 41296, Sweden;* orcid.org/0000-0002-5991-7863; Email: balb@chamlers.se

Amar H. Flood − *Department of Chemistry, Indiana University, Bloomington, Indiana 47405, United States;* orcid.org/0000-0002-2764-9155; Email: aflood@iu.edu

Authors

Fredrik Edhborg − *Department of Chemistry and Chemical Engineering, Chalmers University of Technology, Gothenburg 41296, Sweden;* orcid.org/0000-0001-5168-2935

Axel Olesund − *Department of Chemistry and Chemical Engineering, Chalmers University of Technology, Gothenburg 41296, Sweden;* orcid.org/0000-0003-1202-7844

Vikrant Tripathy − *Department of Chemistry, Indiana University, Bloomington, Indiana 47405, United States;* orcid.org/0000-0002-3246-0680

Yang Wang − *Nano-Science Center & Department of Chemistry, University of Copenhagen, Copenhagen 2100, Denmark;* orcid.org/0000-0003-0867-2752

Tumpa Sadhukhan − *Department of Chemistry, Indiana University, Bloomington, Indiana 47405, United States; Department of Chemistry, SRM Institute of Science and Technology, Chennai 603203, India*

Andrew H. Olsson − *Department of Chemistry, Indiana University, Bloomington, Indiana 47405, United States*

Niels Bisballe − *Nano-Science Center & Department of Chemistry, University of Copenhagen, Copenhagen 2100, Denmark;* orcid.org/0000-0002-4476-5481

Krishnan Raghavachari − *Department of Chemistry, Indiana University, Bloomington, Indiana 47405, United States;* orcid.org/0000-0003-3275-1426

Bo W. Laursen − *Nano-Science Center & Department of Chemistry, University of Copenhagen, Copenhagen 2100, Denmark;* orcid.org/0000-0002-1120-3191

Complete contact information is available at: https://pubs.acs.org/10.1021/acs.jpca.3c02701

Notes

The authors declare no competing financial interest.

■ ACKNOWLEDGMENTS

A.H.F. and K.R. thank the National Science Foundation for support (DMR-2118423). B.A. is grateful to the Swedish Energy Agency (46526-1) and Swedish Research Council for providing financial support. B.W.L. thanks the Danish Council of Independent Research (DFF-0136-00122B). Y.W. thanks the European Union's Horizon 2020 research and innovation programme under the Marie Skłodowska-Curie grant agreement no. 801199.

■ REFERENCES

(1) Lakowicz, J. R. *Principles of Fluorescent Spectroscopy*; Springer, 2006.

(2) Beery, D.; Schmidt, T. W.; Hanson, K. Harnessing Sunlight via Molecular Photon Upconversion. *ACS Appl. Mater. Interfaces* **2021**, *13*, 32601−32605.

(3) Hanna, M. C.; Nozik, A. J. Solar conversion efficiency of photovoltaic and photoelectrolysis cells with carrier multiplication absorbers. *J. Appl. Phys.* **2006**, *100*, 074510.

(4) Di, D.; Romanov, A. S.; Yang, L.; Richter, J. M.; Rivett, J. P. H.; Jones, S.; Thomas, T. H.; Abdi Jalebi, M.; Friend, R. H.; Linnolahti, M.; et al. High-performance light-emitting diodes based on carbene-metal-amides. *Science* **2017**, *356*, 159−163.

(5) Kimura, K.; Miwa, K.; Imada, H.; Imai-Imada, M.; Kawahara, S.; Takeya, J.; Kawai, M.; Galperin, M.; Kim, Y. Selective triplet exciton formation in a single molecule. *Nature* **2019**, *570*, 210−213.

(6) Smith, M. B.; Michl, J. Singlet Fission. *Chem. Rev.* **2010**, *110*, 6891−6936.

(7) Beery, D.; Wheeler, J. P.; Arcidiacono, A.; Hanson, K. CdSe Quantum Dot Sensitized Molecular Photon Upconversion Solar Cells. *ACS Appl. Energy Mater.* **2019**, *3*, 29−37.

(8) Cheng, Y. Y.; Nattestad, A.; Schulze, T. F.; MacQueen, R. W.; Fuckel, B.; Lips, K.; Wallace, G. G.; Khoury, T.; Crossley, M. J.; Schmidt, T. W. Increased upconversion performance for thin film solar cells: a trimolecular composition. *Chem. Sci.* **2016**, *7*, 559−568.

(9) Simpson, C.; Clarke, T. M.; MacQueen, R. W.; Cheng, Y. Y.; Trevitt, A. J.; Mozer, A. J.; Wagner, P.; Schmidt, T. W.; Nattestad, A. An intermediate band dye-sensitised solar cell using triplet-triplet annihilation. *Phys. Chem. Chem. Phys.* **2015**, *17*, 24826−24830.

(10) Börjesson, K.; Dzebo, D.; Albinsson, B.; Moth-Poulsen, K. Photon upconversion facilitated molecular solar energy storage. *J. Mater. Chem. A* **2013**, *1*, 8521.

(11) Yang, Z. Y.; Mao, Z.; Xie, Z. L.; Zhang, Y.; Liu, S. W.; Zhao, J.; Xu, J. R.; Chi, Z. G.; Aldred, M. P. Recent advances in organic thermally activated delayed fluorescence materials. *Chem. Soc. Rev.* **2017**, *46*, 915−1016.

(12) Hill, S. P.; Dilbeck, T.; Baduell, E.; Hanson, K. Integrated Photon Upconversion Solar Cell via Molecular Self-Assembled Bilayers. *ACS Energy Lett.* **2016**, *1*, 3−8.

(13) Singh-Rachford, T. N.; Castellano, F. N. Photon upconversion based on sensitized triplet-triplet annihilation. *Coord. Chem. Rev.* **2010**, *254*, 2560−2573.

(14) Mongin, C.; Moroz, P.; Zamkov, M.; Castellano, F. N. Thermally activated delayed photoluminescence from pyrenyl-functionalized CdSe quantum dots. *Nat. Chem.* **2018**, *10*, 225−230.

(15) Wei, P.; Zhang, X.; Liu, J.; Shan, G. G.; Zhang, H.; Qi, J.; Zhao, W.; Sung, H. H.; Williams, I. D.; Lam, J. W. Y.; et al. New Wine in Old Bottles: Prolonging Room-Temperature Phosphorescence of Crown Ethers by Supramolecular Interactions. *Angew. Chem., Int. Ed.* **2020**, *59*, 9293−9298.

(16) Bock, H. G.-H.; Gharagozloo-Hubmann, K.; Sievert, M.; Prisner, T.; Havlas, Z.; Havlas, Z. Single crystals of an ionic anthracene aggregate with a triplet ground state. *Nature* **2000**, *404*, 267−269.

(17) Dexter, D. L.; Schulman, J. H. Theory of Concentration Quenching in Inorganic Phosphors. *J. Chem. Phys.* **1954**, *22*, 1063−1070.

(18) Chen, R. F.; Knutson, J. R. Mechanism of fluorescence concentration quenching of carboxyfluorescein in liposomes-Energy transfer to nonfluorescent dimers. *Anal. Biochem.* **1988**, *172*, 61−77.

(19) Kasha, M.; Rawls, H. R.; Ashraf El-Bayoumi, M. The exciton model in molecular spectroscopy. *Pure Appl. Chem.* **1965**, *11*, 371−392.

(20) Chaudhuri, K. D. Concentration quenching of fluorescence in solutions. *Z. Phys.* **1959**, *154*, 34−42.

(21) Zhang, X.; Chen, Z. J.; Wurthner, F. Morphology Control of Fluorescent Nanoaggregates by Co-Self-Assembly of Wedge- and Dumbbell-Shaped Amphiphilic Perylene Bisimides. *J. Am. Chem. Soc.* **2007**, *129*, 4886−4887.

(22) Bialas, D.; Zitzler-Kunkel, A.; Kirchner, E.; Schmidt, D.; Wurthner, F. Structural and quantum chemical analysis of exciton coupling in homo- and heteroaggregate stacks of merocyanines. *Nat. Commun.* **2016**, *7*, 12949.

(23) Benson, C. R.; Kacenauskaite, L.; VanDenburgh, K. L.; Zhao, W.; Qiao, B.; Sadhukhan, T.; Pink, M.; Chen, J.; Borgi, S.; Chen, C.-H.; et al. Plug-and-Play Optical Materials from Fluorescent Dyes and Macrocycles. *Chem* **2020**, *6*, 1978−1997.

(24) Chen, J.; Fateminia, S. M. A.; Kacenauskaite, L.; Baerentsen, N.; Gronfeldt Stenspil, S.; Bredehoeft, J.; Martinez, K. L.; Flood, A. H.; Laursen, B. W. Ultrabright Fluorescent Organic Nanoparticles Based on Small-Molecule Ionic Isolation Lattices. *Angew. Chem., Int. Ed. Engl.* **2021**, *60*, 9450−9458.

(25) Chen, J. S.; Stenspil, S. G.; Kaziannis, S.; Kacenauskaite, L.; Lenngren, N.; Kloz, M.; Flood, A. H.; Laursen, B. W. Quantitative Energy Transfer in Organic Nanoparticles Based on Small-Molecule Ionic Isolation Lattices for UV Light Harvesting. *ACS Appl. Nano Mater.* **2022**, *5*, 13887−13893.

(26) Kacenauskaite, L.; Stenspil, S. G.; Olsson, A. H.; Flood, A. H.; Laursen, B. W. Universal Concept for Bright, Organic, Solid-State Emitters-Doping of Small-Molecule Ionic Isolation Lattices with FRET Acceptors. *J. Am. Chem. Soc.* **2022**, *144*, 19981−19989.
(27) Haketa, Y.; Sasaki, S.; Ohta, N.; Masunaga, H.; Ogawa, H.; Mizuno, N.; Araoka, F.; Takezoe, H.; Maeda, H. Oriented salts: dimension-controlled charge-by-charge assemblies from planar receptor-anion complexes. *Angew. Chem., Int. Ed. Engl.* **2010**, *49*, 10079−10083.
(28) Lee, S.; Chen, C. H.; Flood, A. H. A pentagonal cyanostar macrocycle with cyanostilbene CH donors binds anions and forms dialkylphosphate [3]rotaxanes. *Nat. Chem.* **2013**, *5*, 704−710.
(29) Saltiel, J.; Charlton, J. L. Essay 14—Cis-Trans Isomerization of Olefins. *Org. Chem.* **1980**, *42*, 25−89.
(30) Zhang, Y.; Wang, K.; Zhuang, G.; Xie, Z.; Zhang, C.; Cao, F.; Pan, G.; Chen, H.; Zou, B.; Ma, Y. Multicolored-fluorescence switching of ICT-type organic solids with clear color difference: mechanically controlled excited state. *Chem.—Eur. J.* **2015**, *21*, 2474−2479.
(31) Grabowski, Z. R.; Rotkiewicz, K.; Rettig, W. Structural Changes Accompanying Intramolecular Electron Transfer- Focus on Twisted Intramolecular Charge-Transfer States and Structures. *Chem. Rev.* **2003**, *103*, 3899−4032.
(32) Goerner, H. Phosphorescence of trans-Stllbene, Stilbene Derivatives, and Stilbene-like Molecules at 77 K. *J. Phys. Chem.* **1989**, *93*, 1826−1832.
(33) Hirsch, B. E.; Lee, S.; Qiao, B.; Chen, C. H.; McDonald, K. P.; Tait, S. L.; Flood, A. H. Anion-induced dimerization of 5-fold symmetric cyanostars in 3D crystalline solids and 2D self-assembled crystals. *Chem. Commun.* **2014**, *50*, 9827−9830.
(34) Fatila, E. M.; Twum, E. B.; Sengupta, A.; Pink, M.; Karty, J. A.; Raghavachari, K.; Flood, A. H. Anions Stabilize Each Other inside Macrocyclic Hosts. *Angew. Chem., Int. Ed.* **2016**, *55*, 14057−14062.
(35) Fatila, E. M.; Twum, E. B.; Karty, J. A.; Flood, A. H. Ion Pairing and Co-facial Stacking Drive High-Fidelity Bisulfate Assembly with Cyanostar Macrocyclic Hosts. *Chem.—Eur. J.* **2017**, *23*, 10652−10662.
(36) Fatila, E. M.; Pink, M.; Twum, E. B.; Karty, J. A.; Flood, A. H. Phosphate-phosphate oligomerization drives higher order co-assemblies with stacks of cyanostar macrocycles. *Chem. Sci.* **2018**, *9*, 2863−2872.
(37) Liu, Y.; Singharoy, A.; Mayne, C. G.; Sengupta, A.; Raghavachari, K.; Schulten, K.; Flood, A. H. Flexibility Coexists with Shape-Persistence in Cyanostar Macrocycles. *J. Am. Chem. Soc.* **2016**, *138*, 4843−4851.
(38) An, B.-K.; Kwon, S. K.; Jung, S. D.; Park, S. Y. Enhanced Emission and Its Switing in Fluorescent Organic Nanoparticles. *J. Am. Chem. Soc.* **2002**, *124*, 14410−14415.
(39) Fadler, R. E.; Flood, A. H. Rigidity and Flexibility in Rotaxanes and Their Relatives: On Being Stubborn and Easy-going. *Front. Chem.* **2022**, *10*, 856173.
(40) Liu, Y.; Sengupta, A.; Raghavachari, K.; Flood, A. H. Anion Binding in Solution: Beyond the Electrostatic Regime. *Chem* **2017**, *3*, 411−427.
(41) Qiao, B.; Hirsch, B. E.; Lee, S.; Pink, M.; Chen, C. H.; Laursen, B. W.; Flood, A. H. Ion-Pair Oligomerization of Chromogenic Triangulenium Cations with Cyanostar-Modified Anions That Controls Emission in Hierarchical Materials. *J. Am. Chem. Soc.* **2017**, *139*, 6226−6233.
(42) Sandros, K.; Haglid, F.; Ryhage, R.; Ryhage, R.; Stevens, R. Transfer of Triplet State Energy in Fluid Systems III. Reversile Energy Transfer. *Acta Chem. Scand.* **1964**, *18*, 2355−2374.
(43) Saltiel, J.; Khalil, G.-E.; Schanze, K. Trans-stilbene Phosphorescence. *Chem. Phys. Lett.* **1980**, *70*, 233−235.
(44) Benson, C. R.; Maffeo, C.; Fatila, E. M.; Liu, Y.; Sheetz, E. G.; Aksimentiev, A.; Singharoy, A.; Flood, A. H. Inchworm movement of two rings switching onto a thread by biased Brownian diffusion represent a three-body problem. *Proc. Natl. Acad. Sci. U.S.A.* **2018**, *115*, 9391−9396.
(45) Giachino, G. G.; Kearns, D. R. Nature of the External Heavy-Atom Effect on Radiative and Nonradiative Singlet−Triplet Transitions. *J. Chem. Phys.* **1970**, *52*, 2964−2974.
(46) Merkel, P. B.; Dinnocenzo, J. P. Thermodynamic energies of donor and acceptor triplet states. *J. Photochem. Photobiol., A* **2008**, *193*, 110−121.
(47) Kovalenko, S. A.; Dobryakov, A. L.; Ioffe, I.; Ernsting, N. P. Evidence for the phantom state in photoinduced cis-trans isomerization of stilbene. *Chem. Phys. Lett.* **2010**, *493*, 255−258.

https://doi.org/10.1021/acs.jpca.3c02701
J. Phys. Chem. A 2023, 127, 5841−5850